Polymer 51 (2010) 46–52

Contents lists available at ScienceDirect

Polymer

journal homepage: www.elsevier.com/locate/polymer

Macro and meso porous polymeric materials from miscible polysulfone/polyimide blends by chemical decomposition of polyimides

Yong Ding*, Benjamin Bikson

PoroGen Corporation, 6C Gill Street, Woburn, MA 01801, USA

ARTICLE INFO

Article history:
Received 19 October 2009
Received in revised form
19 November 2009
Accepted 21 November 2009
Available online 26 November 2009

Keywords:
Polysulfone
Meso porous
Polyimide

ABSTRACT

Novel macro and meso porous polysulfone materials were prepared from miscible blends of polysulfones with a phenylindane containing polyimide by selective chemical decomposition of the polyimide phase using a dilute hydrazine or tetraammonium hydroxide solution in methanol. It was found that the pore size of the material is affected by the backbone structure of the polysulfone selected. The compatibility between the polysulfones and the polyimide is influenced by the polysulfone structure. This in turn affects the pore size and the pore size distribution of the final porous material. Polyether sulfone was found to form most compatible blends that in turn leads to a porous material with the smallest pore size, a meso porous material. The meso porous polyether sulfones are transparent films, with uniform pore sizes in the range of 30 nm, while bisphenol A polysulfone based porous materials are opaque with pore sizes in the range of 200 nm.

1. Introduction

High specific surface area macro and meso porous materials are increasingly important to understanding, creating, and improving materials for a large number of diverse applications, such as catalytic surfaces and supports, separation and adsorption media, biomaterials, chromatographic materials, etc. [1–3] A typical example is the ordered meso porous inorganic material MCM-41. MCM-41, with pore size in the range of 10–100 nm, is formed by blending a silicate source, such as tetraethoxysilane, with an ionic surfactant under appropriate polymerization conditions [4,5]. MCM-41 is now widely utilized in removal of ultrafine contaminants [5]. Macro porous materials typically contain pores with diameter greater than 50 nm, while meso porous materials are usually defined as those with pore diameter in the range of 2–50 nm [3]. Macro and meso porous polymers with controlled pore size have been synthesized by colloid templating [2,6–9], ion-track etching [10], chemically induced phase separation [11,12], block copolymer self-assembly combined with phase inversion [13–16], selective decomposition of one component of a block copolymer [14,17–31], blending with small molecular weight porogens [32–35], and copolymerization in the presence of porogens [36]. Most of these methods, however, still have some limitations. For example, many of the procedures employed do not generate free-standing porous films or do not completely expose all pores within the material. Phase inversion method has been used extensively for the preparation of porous membranes [37]. The membranes thus obtained are frequently asymmetric with graded pore size across the cross section. Such membranes are frequently mechanically weak and the amount of open pore space on the surface of the membrane as a fraction of the available surface area is relatively small [38].

Our objective was to develop a simple, reliable and industrially feasible process for the fabrication of macro and meso porous membranes with the following key features: (1) a uniform pore size distribution; (2) a three dimensional interconnected network of channels in the bulk; (3) a high specific surface area. It is well documented that the self-assembly of polymers in polymer blends can provide a co-continuous, nano-phase separated system [39]. Such miscible polymer blends offer the potential for the fabrication of porous polymer films by selectively removing one of the components. However, a practical application of this methodology has been limited due to the difficulty of selecting a solvent that removes one of the high molecular weight components quantitatively [40–42]. Herein we detail our approach using polyimide blends as precursor system for preparation of macro and meso porous systems. The rationale is as follows: (1) polyimides can be decomposed with diluted hydrazine into small molecules that in turn can be easily removed; (2) the large library of polyimide structures offers a resource for the formation of compatible and incompatible polyimide blends, which in turn offers the opportunity for tuning the pore structure. The fact that polyimides can be

* Corresponding author. Tel.: +1 11 781 491 0807.
E-mail address: yding@porogen.com (Y. Ding).

0032-3861/$ – see front matter © 2009 Elsevier Ltd. All rights reserved.
doi:10.1016/j.polymer.2009.11.043

quantitatively decomposed by the hydrazine suggests that the removal of the polyimide phase from the blend can be conveniently carried out. By selecting a high performance engineering polymer as the second component of the blend, a porous film with high temperature capability and excellent mechanical properties can be obtained.

In this paper, the new strategy is demonstrated by utilizing polysulfone blends with a commercial phenylindane containing polyimide, Matrimid®. Matrimid® has been reported to form miscible blends with both polyether sulfone (PES) and polysulfone (PSF). [43–45] The structure of precursor polymers used to prepare the blends in this study is shown in Fig. 1. Several novel macro and meso porous polysulfone materials were prepared by selectively removing the polyimide phase from the blend. The influence of the backbone structure of the polysulfone on the blend miscibility and the morphology of the porous materials formed were further studied.

2. Experimental section

2.1. Instruments

ATR FT-IR spectra were recorded on a Nicolet Avatar 360 FT-IR instrument equipped with an Omni-ATR attachment. Differential Scanning Calorimetry (DSC) data were obtained with a Seiko DSC 6200 instrument under nitrogen atmosphere. The heating rate was 10° C/min. The pore size distribution and the total surface area of the macro porous films were determined by Porous Materials, Inc., Ithaca, N. Y., using the mercury intrusion porosimetry method. Cumulative pore volumes and the distribution function $\Delta V/\Delta\log(r)$ was used to express the pore size distribution, where ΔV is the pore volume change when the radius of a cylindrical pore was changed from r to $r - \Delta r$. Field emission scanning electron micrographs (FE-SEM) were obtained on an ISI DS 130 SEM instrument by Analytic Answers, Inc. The cross sections of porous films were prepared by the freeze fracture in liquid nitrogen.

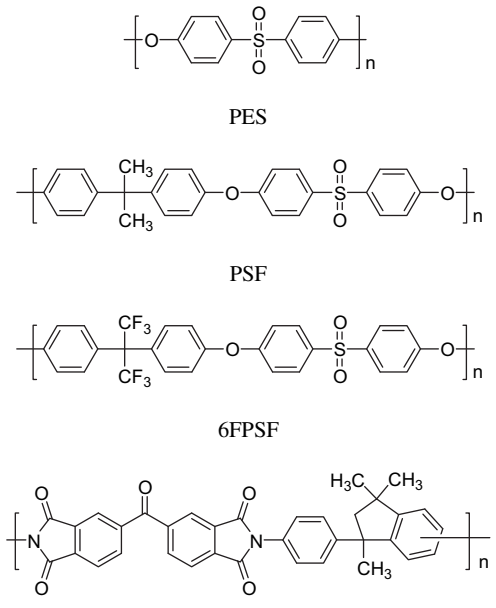

Fig. 1. The structure of polymers utilized in blend preparation.

2.2. Materials

All solvents were purchased from Aldrich and used as received. The commercial phenylindane containing polyimide, Matrimid® 5218, was obtained from Ciba–Geigy. Polyether sulfone, Ultrason® E3010, was purchased form BASF. Polysulfone, Udel® 3500, was purchased from Amoco. Hydrazine monohydrate and tetraammonium hydroxide were obtained from Aldrich Chemicals, Inc.

2.3. Synthesis of 6FPSF

A 1 L three neck flask equipped with a nitrogen inlet, a thermometer, a mechanic stirrer, a Dean Stark trap and a condenser was charged with 67.25 g (0.2 mol) of 4,4′-(hexafluoroisopropylidene)diphenol (6FBPA), 57.43 g (0.2 mol) of dichlorophenylsulfone, 500 mL of NMP, 38.7 g of anhydrous K_2CO_3, and 150 mL of toluene. The mixture was heated to reflux under nitrogen atmosphere with a silicon oil bath and the water formed was removed with the Dean Stark trap. Once the water was totally removed (about 2 h), toluene was then gradually removed and the temperature was raised to 194 °C and kept at this temperature for 4 h. The viscous solution was then cooled down and a fibrous polymer was isolated by precipitation into a large amount of methanol. The polymer was then further purified by washing with excess amount of warm water, and finally with excess amount of methanol. The inherent viscosity of this polymer was 0.49 dL/g, measured at 25 °C with polymer solution concentration of 0.4 g/dL in methylene chloride.

2.4. Preparation of PSF/PI and 6FPSF/PI blend films

Polysulfone/polyimide and 6FPSF/polyimide blend films 50/50 by weight were cast from chloroform solutions (concentration 5% w) using the ring technique described by Moe et al. [46]. The films were dried under vacuum at 160 °C for 48 h. The film diameter was 15 cm and the thickness ca. 0.07 mm.

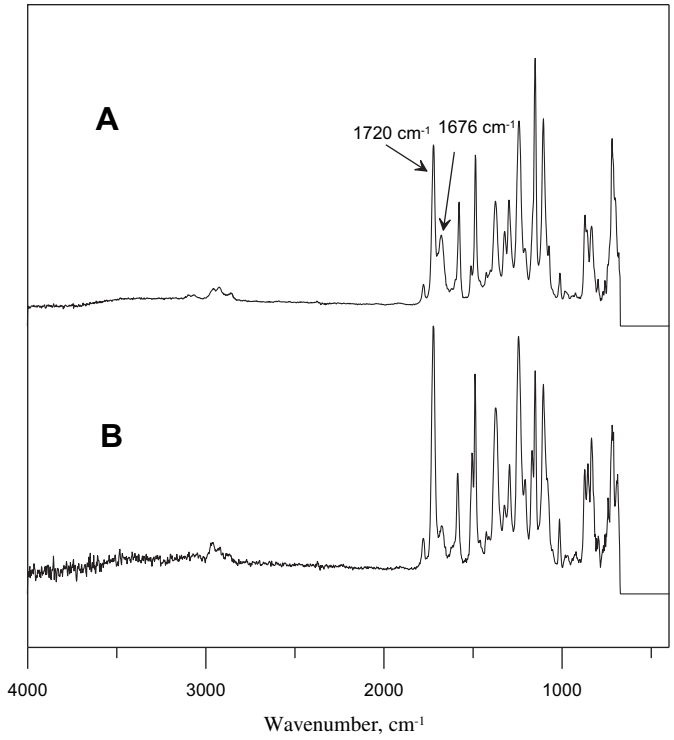

Fig. 2. ATR FT–IR spectra of the PES/PI and PSF/PI blends. A) PES/PI blend, 50/50 by weight; B) PSF/PI blend, 50/50 by weight.

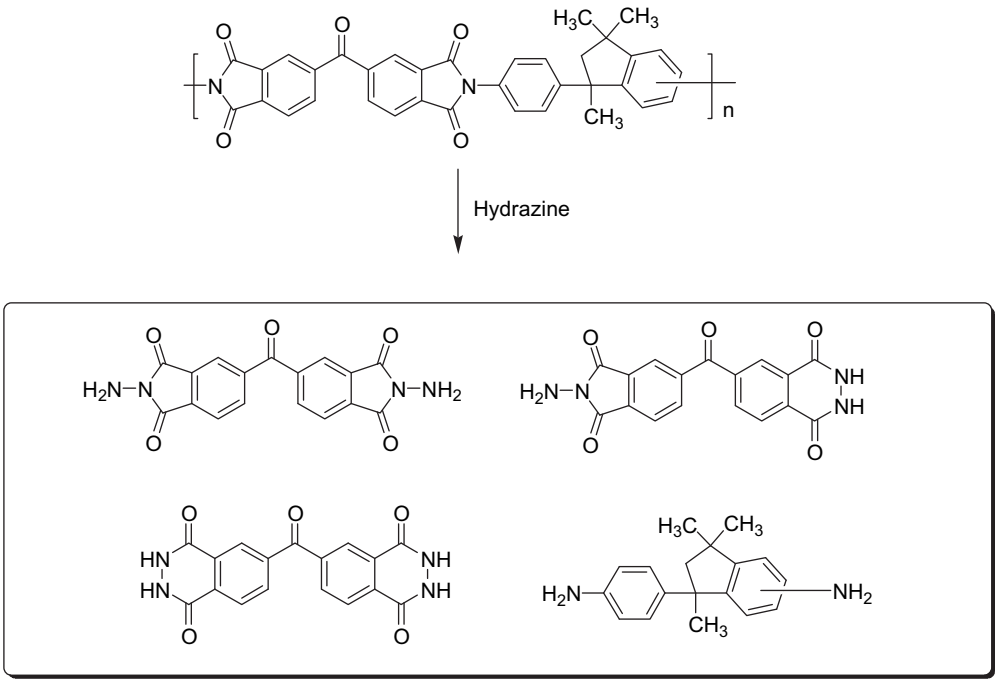

Fig. 3. Decomposition of the phenylindane containing polyimide by the hydrazine.

2.5. Preparation of PES/PI blend films

Polyethersulfone/polyimide blend films 50/50 by weight were cast from NMP (ca. 10% solid) in an oven set at 70 °C using the ring technique described by Moe et al. [46]. The films were then released from the glass plates and dried under vacuum at 160 °C for 48 h. The films were transparent and yellowish. The film diameter was 15 cm and the thickness was ca. 0.07 mm.

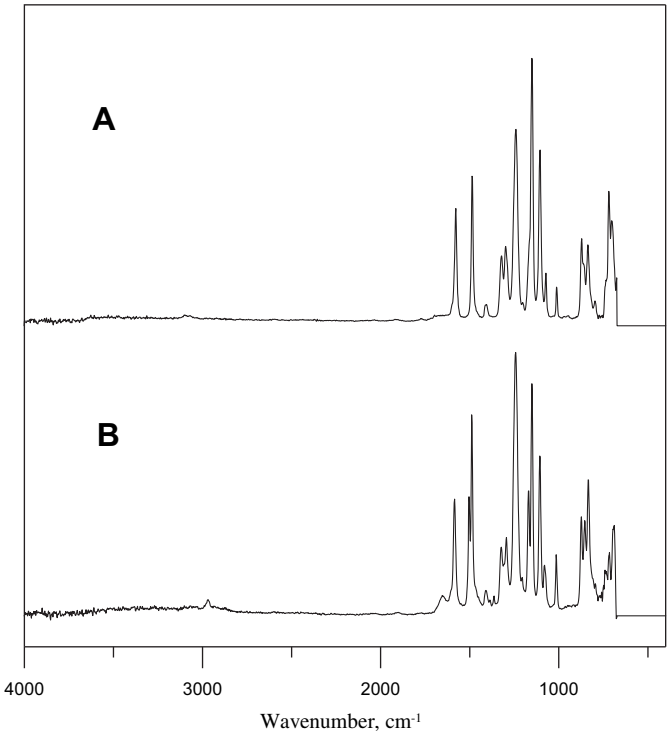

Fig. 4. ATR FT–IR spectra of macro porous materials. A) porous PES film; B) porous PSF film.

2.6. Preparation of porous films

The preparation of the macro porous PSF film provides a representative example of the preparation methodology. A section of a transparent yellowish PSF/PI blend film (15 cm in diameter) was placed into a methanol bath containing 300 mL of methanol and 7 mL of hydrazine monohydrate set at 50 °C. After 5 h, the polyimide was decomposed and small molecular fragments were extracted. A yellowish solution was decanted and 300 mL of fresh methanol containing 5 mL of hydrazine was added and the treatment continued for 2 h. An opaque, white porous polysulfone film was thus obtained, the film was washed with a large excess of methanol and dried under vacuum at room temperature to a constant weight.

2.7. Gas permeation measurements

The permeance of He, O_2 and N_2 through the porous films was measured with a Millipore permeation cell using a bubble tube technique at room temperature (22 °C). The feed gas pressure was 1.3 bar and the down stream pressure was 1.01 bar. The membrane area was 14.5 cm^2.

3. Results and discussion

3.1. PES and PSF blends with the phenylindane containing polyimide

Three polysulfone blends were chosen in this initial study to demonstrate the methodology of formation of macro and meso porous films. Films of polymer blends were cast from solutions of the phenylindane containing polyimide with PES, PSF, and 6FPSF, respectively. It is essential that the polymer blends form co-continuous phases. To form interconnected phases, the polyimide

Table 1
Physical changes of films upon removal of the polyimide phases.

Porous film	Weight change (%)	Dimensional changes (%)		
		Length	Thickness	Volume
PES	−50.0	−4.8	−4.5	−12.5
PSF	−50.0	0	−7.3	−7.3

content of blends can vary from about 16% to about 84% by volume based on the classic percolation theory [47]. The concentration of the polyimide phase in the precursor will affect the pore size and the pore size distribution in the final porous film. However, in this initial study we report on preparation of 50/50 blends by weight only and porous films formed therefrom. The blends can be formed into variable shaped devices by melt or solution processing. In this study, polymer blend films were prepared by solution casting.

Transparent, yellowish films were obtained from PES or PSF blends, an indication of a partial or complete miscibility. 6FPSF/polyimide blends formed tough films. However, films were opaque, an indication that the blends were largely immiscible. Only one glass transition temperature was observed for PES and PSF blends by DSC study, which is consistent with literature findings that the phenylindane containing polyimide forms miscible blends with PES and PSF [43–45]. However, two distinct glass transition temperatures were observed for the 6FPSF blend, a confirmation that the 6FPSF and the phenylindane containing polyimide were immiscible. Since 6FPSF did not form a miscible blend with the phenylindane containing polyimide, further study of the 6FPSF polyimide blend was discontinued.

The ATR-FTIR spectra of the PES and the PSF blends are shown in Fig. 2. Both spectra exhibit characteristic peaks at 1720 and 1676 cm^{-1}, assigned to the –CO- group in the imide linkage. A comparison between the two figures shows that the peak at 1720 cm^{-1} in the PES/PI blend is weaker than the 1720 cm^{-1} peak in the PSF/PI blend. On the other hand, the peak at 1676 cm^{-1} in the PES/PI blend is much stronger than the corresponding peak in the PSF/PI blend. The increase in 1676 cm^{-1} peak intensity can be attributed to the frequency shift of the peak at 1720 cm^{-1}, due to specific interactions between the characteristic groups of component polymers. The higher intensity ratio of the peak at 1676 cm^{-1} to that at 1720 cm^{-1} peak for the PES/PI blend as compared to that of the PSF/PI blend suggests that the PES/PI blend is more miscible. This has been confirmed by a subsequent observation of differences in pore sizes between porous materials formed from these blends.

3.2. Formation of macro and meso porous films

A polyimide can be decomposed into small molecules by hydrazine due to the fact that the hydrazine can replace the aromatic amines in the polymer chain [48]. The decomposition of the polyimide by hydrazine is schematically shown in Fig. 3. Methanol was selected as the solvent to carry out the reaction. Since methanol is a non solvent for most high performance polymers, including polysulfones and polyimides, it was expected that the exposure to methanol will not result in swelling and a change in the blend morphology. Small molecular fragments formed after the decomposition of the polyimide are soluble in methanol, and can be extracted, leaving the pores behind. To enhance the solubility of molecular fragments in methanol and accelerate the extraction, elevated temperatures were employed. The similar results were obtained by using tetraammonium hydroxide, a strong organic base.

The removal of the polyimide phase from blends can be followed visually. The PSF/PI and PES/PI blends are yellowish in color. After the removal of the polyimide, the yellowish color disappears. ATR FT-IR spectra confirmed the complete removal of the polyimide. The ATR FT-IR spectra of the porous PES and PSF films are shown in Fig. 4. It can be seen that the characteristic stretching vibration of the –CO- group (1720 cm^{-1} and 1676 cm^{-1}) of the polyimide is absent in both the PES and the PSF film spectra. This suggests that the final PES and PSF films do not have any polyimide content remaining.

The complete removal of the PI has been also confirmed by the gravimetric analyses. The sample weight changes are summarized in Table 1. The dimensional changes in films after the removal of the polyimide phase are also summarized in Table 1. The percentage weight loss for both PSF and PES films is consistent with the quantitative removal of the polyimide phase.

There are small changes in dimensions between the precursor film and the porous film. The width and length of the porous PES film are 95.2% of those of the precursor film and thickness is 95.5% of that of the precursor film. The width and length of the porous PSF film are the same as those of the precursor film. However, the thickness of the porous PSF film is 93.7% of that of the precursor film. Overall, the porous PES film shrunk slightly more than the porous PSF film did.

The PSF porous films are white in color and opaque. In contrast, the PES porous films are colorless and transparent. A photograph of a piece of the PES porous film is shown in Fig. 5. For comparison, a photograph of a piece of the PES/PI blend film is also shown in Fig. 5. The films have been photographed against a background to

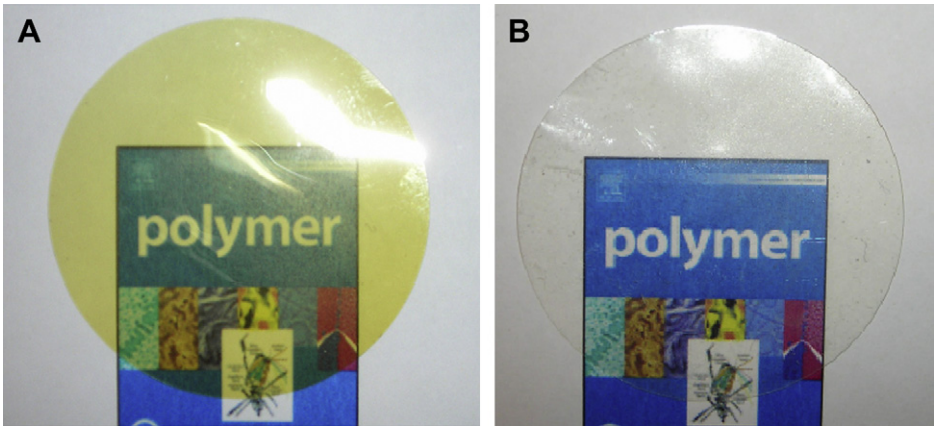

Fig. 5. Photographs of a piece of the PES/PI blend film and a piece of the meso porous PES film obtained therefrom. (A)the PES/PI (50/50) blend film (B) the meso porous PES film.

highlight the transparency. It can be seen that after the polyimide removal, the porous PES film is still clear and transparent. Qualitatively, the porous films appear to retain the handling characteristics of the nonporous precursors, such as flexibility and creasibility.

3.3. Characterization of macro porous films

The FE-SEM micro photograph of a cross section and of the surface of the PES porous film are shown in Fig. 6. The microphotographs show that the pores in the PES film are largely cylindrically shaped and interconnected. The pore size is uniform, with the pore diameter averaging around 30 nm.

The FE-SEM microphotographs of a cross section and of the surface of the PSF macro porous film are shown in Fig. 7. These microphotographs show that the pores in the PSF film are largely cylindrically shaped as well and interconnected. The pore size is uniform, with the pore diameter averaging around 200 nm.

The difference in pore sizes between PES and PSF films is consistent with the different physical appearance of the two porous films, i.e., PES films are transparent while PSF films are opaque. The pore size of the PSF film is 6 times as large as that of the PES film, and exceeds the threshold required for transparency. The results also suggest that PES forms a more compatible blend with the phenylindane containing polyimide than the PSF does, which is consistent with the results of the FT-IR analysis discussed above.

We have also studied the distribution and the size of pores by the mercury intrusion porosimetry. The experimental results are shown in Fig. 8. It can be seen that both the PES and PSF porous films exhibit a relatively narrow pore size distribution, with mean pore size of 30 nm for the PES material and mean pore size of 200 nm for the PSF material. The results are in a good agreement with that obtained by SEM measurements and allow us to classify the PES and PSF porous films as meso porous and macro porous, respectively. The mercury intrusion isotherms for both films exhibit a step increase in the mercury intrusion isotherm due to the capillary surface tension at a certain mercury pressure. This strongly suggested that the pores in both the PES and the PSF porous films are ordered. The mercury intrusion porosimetry is inadequate to analyze pores with pore diameter smaller than 3.5 nm [49]. Additional techniques, such as the nitrogen adsorption/desorption method, must be employed to determine whether micro size pores are further present in the matrix, a characteristic common to many porous inorganic systems [50,51].

An important characteristic of macro and meso porous materials is the net void volume, or the specific surface area, of the system. The PES meso porous material exhibited a specific surface area of 123 m^2/g and the PSF macro porous material exhibited a specific surface area of 175 m^2/g, as measured by mercury intrusion porosimetry. The methodology utilized does not measure micro size pores and thus may not reflect the true total specific surface area, in particular for PES materials that has smaller size pores. The

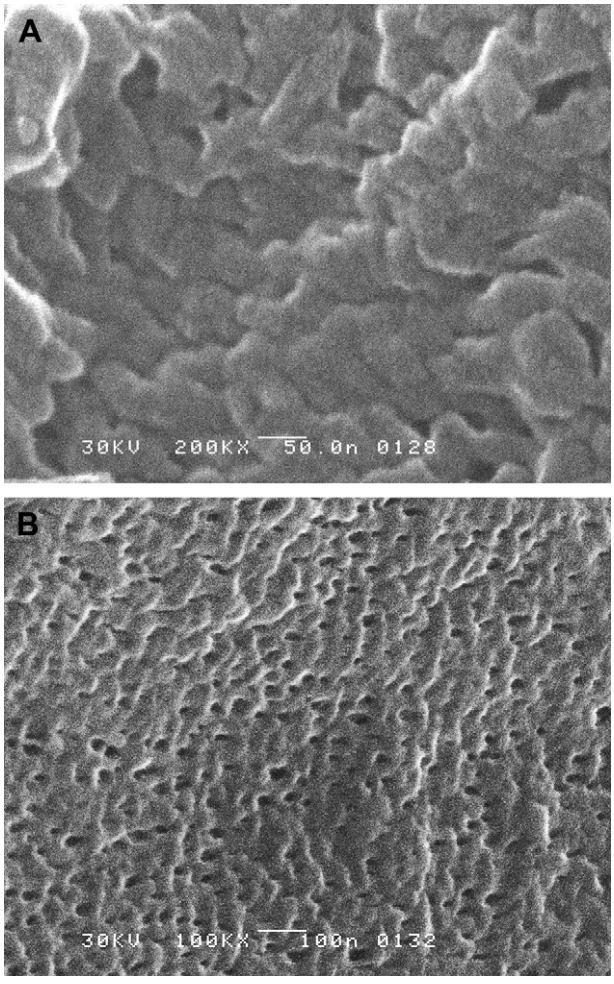

Fig. 6. FE-SEM images of the meso porous PES film. (A) the cross section; (B) the surface.

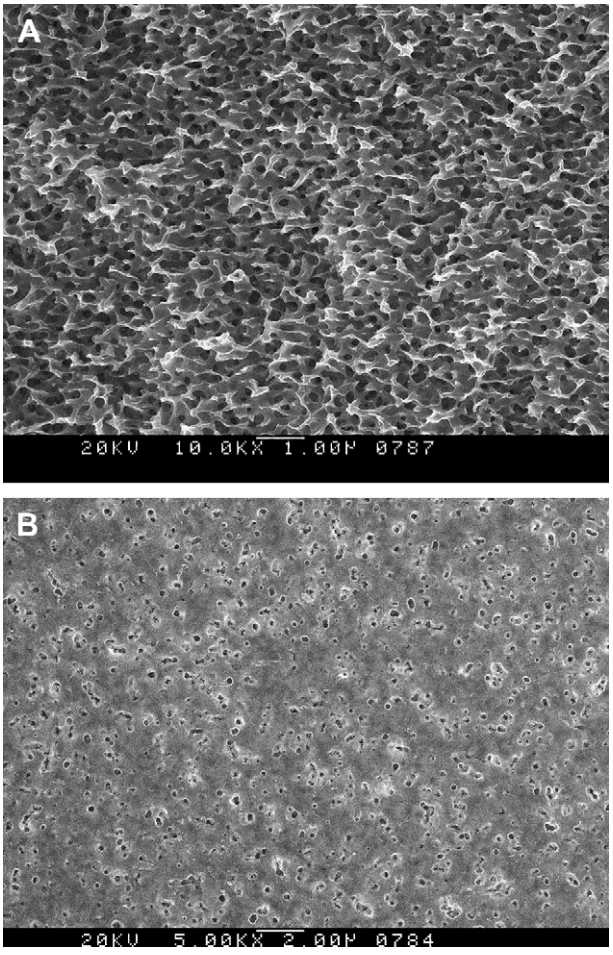

Fig. 7. FE-SEM images of the macro porous polysulfone film. (A) the cross section; (B) the surface.

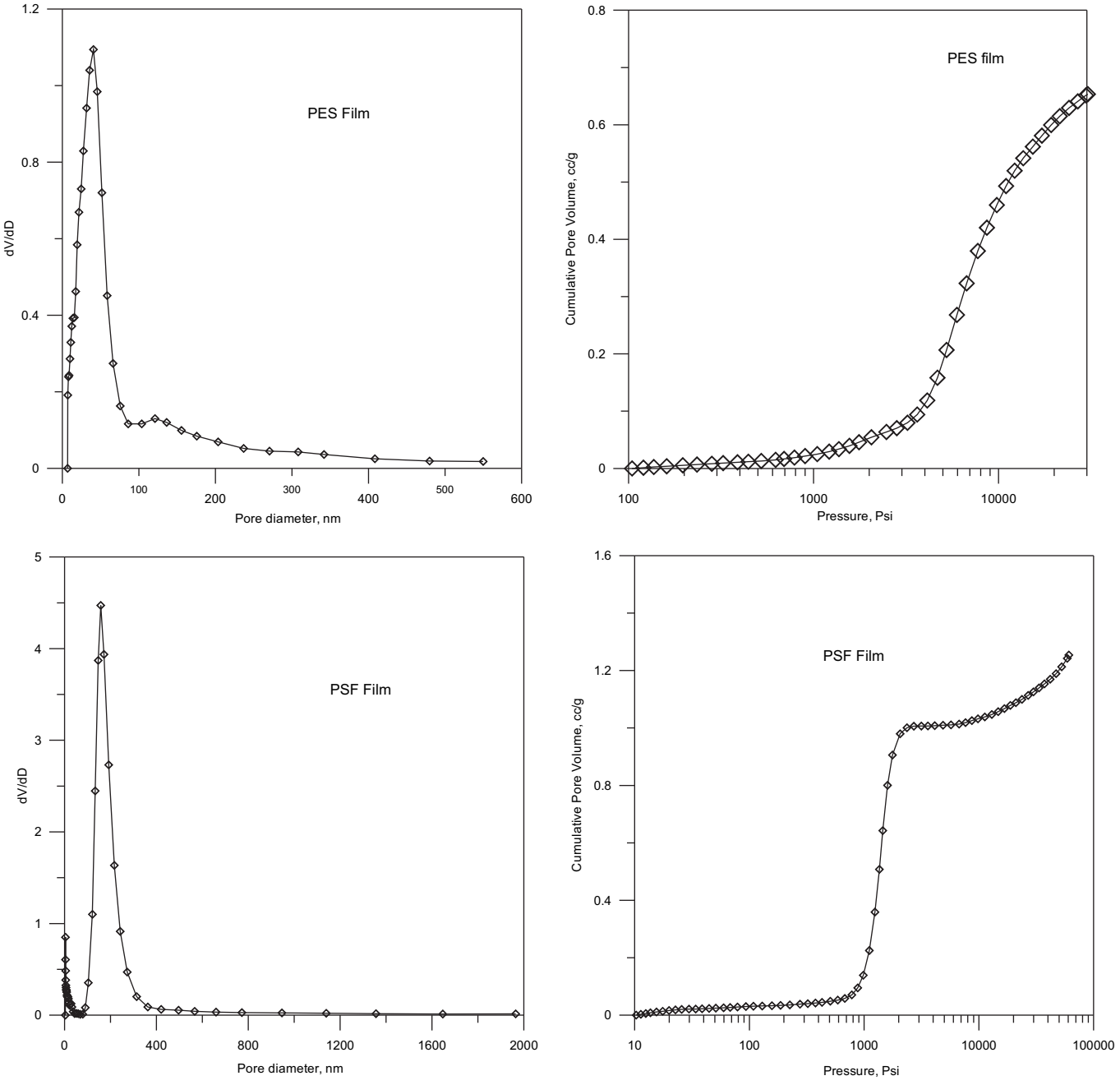

Fig. 8. Pore size distribution of the PES and the PSF porous films by the mercury intrusion porosimetry.

slightly smaller specific surface area of the PES meso porous material may be also due to the collapse of the smallest size pores during drying. It is known that the drying procedure can affect the final porosity of the material. However, in this initial study, the drying methodology has not been optimized to maximize the specific surface area. A slightly higher shrinkage of the porous PES film as compared to the porous PSF film is consistent with this hypothesis.

The measured gas transport characteristics of porous PES and PSF films provided further evidence that the pores in the bulk are interconnected. The gas transport of a porous membrane is characterized by its permeance. The permeance is defined as follows:

$$P/l = J/(p_h - p_l) \quad (1)$$

where P/l is the permeance, which is the pressure normalized flux, P is the permeability coefficient, l is the membrane thickness, J is the flux, and p_h and p_l are partial pressures of the gas on the feed and the permeate side. Ideal selectivity for two gases A and B is defined as:

Table 2
Gas transport characteristics of the PES and the PSF porous films.

Porous film	Permeance[a]			Selectivity	
	He	O_2	N_2	α (O_2/N_2)	α (He/N_2)
PES	2800	970	1100	0.92	2.6
PSF	6400	4300	4800	0.91	1.3

[a] The unit of the permeance is 10^{-5} cm^3/cm^2.cmHg.sec.

$$\alpha = \frac{(P/l)_A}{(P/l)_B} \quad (2)$$

The measured gas transport characteristics of the PES and the PSF porous films are summarized in Table 2. Both porous films exhibited very high permeances for all gases measured. The high permeance for both films confirmed that the pores are interconnected. The PSF film exhibited a slightly higher gas permeance as compared to the PES film, combined with a slightly lower separation factor. The PES film exhibited gas separation factors that are close to the ideal Knudsen flow, which is 2.65 for the He/N_2 gas pair and 0.94 for the O_2/N_2 gas pair. These results are consistent with the previous finding that the pore size of the meso porous PES film was much smaller than that of the macro porous PSF film.

4. Conclusions

A novel method for the fabrication of macro and meso porous materials with uniform pore sizes was developed. The method is industrially feasible and can be utilized to fabricate large area devices of variable shapes. The success of this method relies on the self-assembly of polymers in miscible blends that form macro or meso co-continuous phases and the ability to remove one of the components, the polyimide, at mild conditions that preserve the porous structure. Two representative porous materials, the polyether sulfone and the bisphenol A polysulfone, were prepared from their blends with the phenylindane containing polyimide. Both films exhibited uniform pore size distribution and pore inter connectivity. The PES meso porous films are transparent with pore sizes in the range of 30 nm. The macro porous PSF based macro materials are opaque with pore sizes in the range of 200 nm. Macro and meso porous films obtained by the novel approach can be useful as membranes for nanoseparations, bioseparations, scafoldings and substrates.

References

[1] Barton TJ, Bull LM, Klemperer WG, Loy DA, McEnaney B, Misono M, et al. Chemistry of Materials 1999;11:2633–56.
[2] Jiang P, Hwang KS, Mittleman DM, Bertone JF, Colvin VL. Journal of the American Chemical Society 1999;121:11630–7.
[3] Wang D, Caruso RA, Caruso F. Chemistry of Materials 2001;13:364–71.
[4] Beck JS, Vartuli JC, Roth WJ, Leonowicz ME, Kresge CT, Schmitt KD, et al. Journal of the American Chemical Society 1992;114:10834–43.
[5] Kresge CT, Leonowicz ME, Roth WJ, Vartuli JC, Beck JS. Nature 1992;359:710.
[6] Ruchenstein E, Zang X. Macroporous or microporous filtration membrane, method of preparation and use. U.S. Patent 5,993,661; 1999.
[7] Park SH, Xia Y. Chemistry of Materials 1998;10:1745–7.
[8] Gates B, Yin Y, Xia Y. Chemistry of Materials 1999;11:2827–36.
[9] Johnson SA, Ollivier PJ, Mallouk TE. Science 1999;283:963–5.
[10] Yoshida M, Asano M, Suwa T, Reber N, Spohr R, Katakai R. Advanced Materials 1997;9:757.
[11] Kiefer J, Hilborn JG, Maanson JAE, Leterrier Y, Hedrick JL. Macromolecules 1996;29:4158.
[12] Mendelsohn JD, Barrett CJ, Chan VV, Pal AJ, Mayers AM, Rubner MF. Langmuir 2000;16:5017–23.
[13] Widawski G, Rawiso M, Francois B. Nature 1994;369:387.
[14] Liu G, Ding J, Hashimoto T, Kimishima K, Winnik FM, Nigam S. Chemistry of Materials 1999;11:2233–40.
[15] Chen Y, Ford WT, Materer NF, Teeters D. Journal of the American Chemical Society 2000;122:10472–3.
[16] Chen Y, Ford WT, Materer NF, Teeters D. Chemistry of Materials 2001;13:2697–704.
[17] Lee J-S, Hirao A, Nakahama S. Macromolecules 1989;22:2602–6.
[18] Koyama K, Ohno S. Porous synthetic resin film. U.S.: Toyo Soda Manufacturing Co., Ltd.; 1978.
[19] Zalusky AS, Olayo-Valles R, Taylor CJ, Hillmyer MA. Journal of the American Chemical Society 2001;123:1519–20.
[20] Liu G, Ding J, Guo A, Herfort M, Bazett-Jones D. Macromolecules 1997;30:1851–3.
[21] Liu G, Ding J, Stewart S. Angewante Chemie, International Edition in English 1999;38:835–8.
[22] Henselwood F, Liu G. Macromolecules 1998;31:4213–7.
[23] Charlier Y, Hedrick JL, Russell TP, Jonas A, Volksen W. Polymer 1995;36:987–1002.
[24] Carter KR, DiPietro RA, Sanchez MI, Swanson SA. Chemistry of Materials 2001;13:213–21.
[25] Hedrick J, Labadie J, Russell T, Hofer D, Wakharker V. Polymer 1993;34:4717.
[26] Plummer CJG, Hedrick JL, Kausch HH, Hilborn JG. Journal of Polymer Science, Polymer Physics 1995;33:1813–20.
[27] Hedrick JL, Hawker CJ, DiPietro R, Jerome R, Charlier Y. Polymer 1995;25:4855–66.
[28] Fodor JS, Briber RM, Russell TP, Carter KR, Hedrick JL, Miller RD. Journal of Polymer Science, Polymer Physics 1997;35:1067–76.
[29] Charlier Y, Hedrick JL, Russell TP, Swanson S, Sanchez M, Jerome R. Polymer 1995;36:1315.
[30] McGrath JE, Jayaraman SK, Lakshmanan P, Abed JC, Afchar-Taromi F. Polymer Preprints 1996;37(1):136–7.
[31] Takeichi T, Guo M, Ito A. High Performance Polymers 1999;11:1–14.
[32] Baniel A, Eyal A, Edelstein D, Hajdu K, Hazan B, Ilan Y, et al. Journal of Membrane Science 1990;54:271–83.
[33] Eyal AM, Hazan B, Hajdu K, Edelstein D. Journal of Applied Polymer Science 1992;45:1065–74.
[34] Eyal AM, Hajdu K, Hazan B, Edelstein D. Journal of Applied Polymer Science 1992;46:1621–9.
[35] Eyal AM, Hajdu K, Hazan B, Edelstein D. Journal of Applied Polymer Science 1992;46:1613–20.
[36] Peters EC, Svec F, Frechet JMJ. Chemistry of Materials 1997;9:1898.
[37] Koros WJ, Fleming CK. Journal of Membrane Science 1993;83:1–80.
[38] Kools W. Method of manufacturing membranes and the resulting membranes. WO: Millipore; 2001.
[39] Paul DR, Newman S. Polymer blends. New York: Academic Press; 1978.
[40] Walheim S, Schaffer E, Mlynek J, Steiner U. Science 1999;283:520.
[41] Li J, Ma PL, Favis BD. Macromolecules 2002;35:2005–16.
[42] Lin W-J, Lu C-H. Journal of Membrane Science 2002;198:109–18.
[43] Liang K, Grebowwicz J, Valles E, Karasz FE, MacKnight WJ. Journal of Polymer Science Polymer Physics 1992;30:465–76.
[44] Kapantaidaski GC, Kaldis SP, Dabou XS, Sakellaropoulos GP. Journal of Membrane Science 1996;110:239–47.
[45] Kapantaidakis GC, Kaldis SP, Sakellaropoulos GP, Chira E, Loppinet B, Floudas G. Journal of Polymer Science Polymer Physics 1999;37:2788–98.
[46] Moe M, Koros WJ, Hoehn HH, Husk GR. Journal of Applied Polymer Science 1988;36:1833.
[47] Stauffer D, Aharony A. Introduction to percolation theory. 2nd ed. London: Taylor and Francis; 1992.
[48] Herbert CC, Ghassemi H, Hay AS. Journal of Polymer Science-Polymer Chemistry Edition 1997;35:1095–104.
[49] Hsieh HP. General characteristics of inorganic membranes. In: Bhave RR, editor. Inorganic membranes: synthesis, characteristics, and applications. New York: Van Nostrand Reinhold; 1991. p. 64–94.
[50] Goltner C, Smarsly B, Berton B, Antonietti M. Chemistry of Materials 2001;13:1617–24.
[51] Samrsly B, Goltner C, Antonietti M, Ruland W, Hoinkis E. The Journal of Physical Chemistry B 2001;105:831–40.